JACC: CARDIOVASCULAR IMAGING
VOL. 3, NO. 1, 2010

ISSN 1936-878X/10/$36.00
PUBLISHED BY ELSEVIER INC.
DOI:10.1016/j.jcmg.2009.09.018

Accuracy of Optical Coherence Tomography in the Evaluation of Neointimal Coverage After Stent Implantation

Akira Murata, MD,* David Wallace-Bradley, BS,* Armando Tellez, MD,* Carlos Alviar, MD,* Michael Aboodi, BS,* Alexander Sheehy, MS,† Leslie Coleman, DVM, MS,† Laura Perkins, DVM, PHD,† Gaku Nakazawa, MD,‡ Gary Mintz, MD,* Greg L. Kaluza, MD, PHD,* Renu Virmani, MD,‡ Juan F. Granada, MD*

Orangeburg, New York; Santa Clara, California; and Gaithersburg, Maryland

OBJECTIVES This study aimed to evaluate the accuracy of optical coherence tomography (OCT) in analyzing the neointimal response to several drug-eluting stent (DES) types by comparing OCT images acquired in vivo with corresponding histological specimens using a nondiseased porcine injury model.

BACKGROUND Optical coherence tomography is emerging as a promising endovascular imaging tool for the evaluation of neointimal response after DES implantation.

METHODS A total of 84 stents were implanted—22 ML Vision (Abbott Vascular, Santa Clara, California), 22 Xience V (Abbott Vascular), 20 Endeavor (Medtronic, Minneapolis, Minnesota), and 20 Taxus Liberté (Boston Scientific, Natick, Massachusetts) stents—in normal porcine coronary arteries and were harvested at 28 ($n = 42$) and 90 ($n = 42$) days, with the different stent types equally distributed between the 2 follow-up periods. At termination, morphometric evaluation using OCT imaging was performed in all stented arteries. Histological morphometric analysis was performed and correlated with OCT.

RESULTS A total of 622 OCT–histology matched frames acquired from all stent designs were analyzed. The luminal (13.7%) and stent (6.1%) areas were consistently larger by OCT compared with histology. The mean neointimal thickness was very similar between techniques (~3.27% variation). There was a high correlation between OCT and histology for the evaluation of neointimal area ($R^2 = 0.804$), luminal area ($R^2 = 0.825$), and neointimal thickness ($R^2 = 0.789$). Correlation for total stent area was poor ($R^2 = 0.352$). Although the proportion of individual struts determined to be uncovered by OCT and histology was similar, there was significant variation in the estimation of strut coverage between OCT and histology when the neointimal thickness was between 20 and 80 μm. This variation converged for neointimal thicknesses between 80 and 100 μm.

CONCLUSIONS Subtle differences in neointimal formation induced by current DES can be reproducibly analyzed in vivo by OCT. However, OCT measurement of stent area seems to have less correlation with histology. (J Am Coll Cardiol Img 2010;3:76–84) © 2010 by the American College of Cardiology Foundation

From the *Skirball Center for Cardiovascular Research, Cardiovascular Research Foundation, Orangeburg, New York; †Abbott Vascular, Santa Clara, California; and ‡CV Path, Gaithersburg, Maryland. This study was partially funded by a research grant provided by Abbott Vascular. Mr. Sheehy, Dr. Coleman, and Dr. Perkins are employees of Abbott Vascular.

Manuscript received April 17, 2009; revised manuscript received September 4, 2009, accepted September 22, 2009.

Drug-eluting stents (DES) reduce the amount of neointimal formation among patients undergoing coronary stent placement (1–3). Recent data indicate that a small yet cumulative risk of late stent thrombosis persists over time (4,5). Human pathology studies suggest that the lack of strut coverage due to delayed vascular healing may be associated with late thrombotic events after DES implantation (6,7). Hence, accurate assessment of neointimal coverage in DES in vivo may be critical in prognosticating their safety and utility.

See page 85

Due to its high resolution, optical coherence tomography (OCT) has emerged as perhaps a promising endovascular imaging technique for the evaluation of neointimal formation after DES implantation (8–13). Despite the fact that preliminary clinical data already have been published (14,15), the accuracy of this technique for the in vivo evaluation of neointimal formation after DES implantation has not been systematically tested. In the present study, we examine the accuracy and operator reproducibility of OCT in quantifying the degree of neointimal coverage using several DES designs by correlating images acquired in vivo with matched histological specimens. We sought to validate the in vivo accuracy of OCT as an imaging modality to examine and measure the neointimal responses to DES implantation.

METHODS

Study design. A total of 28 purpose-bred Yorkshire swine, weighing 25 to 35 kg, were used in the present study. The study protocol was approved by the local institutional animal care and use committee. All animals received humane care in compliance with the Animal Welfare Act and the Principles of Laboratory Animal Care formulated by the Institute of Laboratory Animal Resources (National Research Council, National Institutes of Health Publication No. 85-23, revised 1996). After stent implantation, all animals were divided into 2 groups according to follow-up length at 28 (n = 14) or 90 days (n = 14) to evaluate different stages of neointimal formation. At the time of deployment, each stent was systematically randomized to implantation into the left anterior descending (LAD), left circumflex (LCX), or right coronary arteries (RCA) of each animal. A total of 84 stents were deployed: ML Vision (3.0 × 12 mm, Abbott Vascular, Santa Clara, California, n = 22), Xience V everolimus-eluting (3.0 × 12 mm, Abbott Vascular, n = 22), Endeavor zotarolimus-eluting (3.0 × 12 mm, Medtronic, Minneapolis, Minnesota, n = 20), or Taxus Liberté paclitaxel-eluting stent (3.0 × 12 mm, Boston Scientific, Natick, Massachusetts, n = 20). The different stent types were equally distributed between the 2 follow-up periods.

Procedural description. Animals were pre-anesthetized with a mixture of glycopyrrolate, Telazol (Fort Dodge Animal Health, Fort Dodge, Iowa), and xylazine based on animal weight. When an adequate anesthetic plane was reached, the animals were intubated and inhaled isoflurane (1% to 2%) delivered through a precision vaporizer and a circle absorption breathing system with periodic arterial blood gas monitoring. Continuous monitoring of vital signs was performed and was recorded at approximately 15-min intervals. A vascular access sheath (7-F) was placed in the carotid artery by cut-down with general sterile technique. Before catheterization, heparin (5,000 to 10,000 IU) was injected to maintain an activated coagulation time of 250 to 300 s. For each stent deployment, an arterial segment was chosen so as to result in a stent-to-artery ratio of ≥1.1. The GE quantitative coronary angiographic (QCA) package (version 4.0.12, GE Medical Systems, Salt Lake City, Utah) was used for these measurements. After vessel allocation to an experimental group, the appropriate stent was delivered to the intended site over a guidewire using fluoroscopic guidance. Stents were deployed in segments devoid of major side branches. After stent implantation, hemostasis was obtained by arterial ligation using 2-0 silk suture, and the incision site was closed in 2 to 3 layers with appropriate suture material. All animals received aspirin (81 mg) and clopidogrel (75 mg) daily and were fed a regular diet throughout the study.

OCT imaging protocol. The OCT images were recorded using the M2 OCT imaging system (LightLab Imaging, Inc., Westford, Massachusetts). The M2 OCT system uses a 1,310-nm broadband light source and the principles of interferometry to produce images with an axial resolution of 15 μm and a lateral resolution of 25 μm. The OCT imaging probe (ImageWire, LightLab Imaging, Inc.) was used to deliver light to the tissue and to collect the reflected signal. The ImageWire consists of a 0.006-inch (0.15-mm) fiberoptic core inside a transparent sheath with a 0.016-inch (0.41-mm) maximum outer diameter (16). Integrated OCT

ABBREVIATIONS AND ACRONYMS

DES = drug-eluting stent(s)
EEL = external elastic lamina
IEL = internal elastic lamina
LAD = left anterior descending
LCX = left circumflex
OCT = optical coherence tomography
QCA = quantitative coronary angiography
RCA = right coronary artery

image analysis software developed by the company was used for all measurements. System calibration of the Z-offset was performed on each image wire before every imaging procedure. Using conventional catheterization techniques, an occlusion catheter was advanced distal to the stented segment on a 0.014-inch (0.36-mm) coronary guidewire. The 0.014-inch guidewire was then exchanged for the OCT imaging wire, and the occlusion device was pulled back to the proximal reference segment. The OCT imaging was performed during balloon occlusion (0.3 atm) using continuous saline flush at a rate of 0.5 to 1.0 ml/s. Motorized OCT pullbacks were performed at a rate of 1.0 mm/s. All images were acquired at 15.6 frames/s and displayed with a color look-up table and digitally archived. If the initial pullback was not of adequate quality, sequential pullbacks were performed until an optimal sequence was achieved. All images were stored on the system hard drive for offline analysis.

OCT imaging analysis. Two skilled operators blinded to the stent type and histological results performed all OCT analyses. Measurements were performed every 1 mm from the distal to the proximal stent segments. The first analyzable frame was defined as the first OCT frame which allowed the drawing of a complete circumference using the strut contour, and was considered the distal stent ending. Every subsequent millimeter was specified by the OCT frame rate, allowing for precise histology–OCT frame registration. Stent area was defined by the evaluator as the circumferential area limited by the contours of the struts. This zone was demarcated by manually placing dots along its inner contour, and an interpolated spline automatically delineated the stent circumference. The lumen area was defined by the evaluator as the leading edge of the circumferential hyper-reflective zone covering the stent struts. This zone was demarcated and its area calculated in a manner identical to that of the stent area. The neointimal area was calculated by subtracting the lumen area from the stent area. To analyze neointimal thickness, the distance between the border of each strut, defined as the axial and lateral center of the stent strut reflection (so-called blooming artifact), and the luminal border was measured in the direction of the stent center of gravity. A strut was considered covered if the amount of neointimal thickness assessed by this method was ≥ 20 μm.

Tissue harvesting and histology protocol. All animals were euthanized immediately after terminal angiography and OCT under general anesthesia using intravenous injection of pentobarbital euthanasia solution (100 mg/kg) and/or potassium chloride (40 mEq). Hearts were excised and pressure-perfused with 0.9% saline until cleared of blood, followed by pressure-perfusion fixation in 10% neutral buffered formalin until hardening of the heart muscle was clearly perceptible. Before histological processing, intact hearts with stented vessels were imaged by capturing high-contrast film-based radiographs (Faxitron X-ray Corp., model 43855A, Lincolnshire, Illinois) to locate and assess stent location. The stented arterial segments were then carefully dissected free from the heart and examined by X-ray. The implanted vessel segments were fixed in 10% formalin, dehydrated in a graded series of ethanol, and embedded in methyl methacrylate resin. After polymerization, sections measuring approximately 1.3 mm were sawed from each stent, beginning at the distal stent edge. Individual slides were cut on a rotary microtome at 4 to 6 μm, mounted, and stained with hematoxylin and eosin and elastic Van Gieson stains. There were no histological sections lost due to processing, and all sections were of excellent quality.

The cross-sectional areas (external elastic lamina [EEL], internal elastic lamina [IEL], and lumen area) of each section were measured using digital morphometry software (IPLab, BD Biosciences, Rockville, Maryland). Neointimal thickness was measured as the distance from the inner surface of each stent strut to the luminal border in the direction of the vessel center of gravity. Area measurements were used to calculate vessel layer areas: media (EEL − IEL), neointima (IEL − lumen), and percent stenosis (1 − (lumen area/IEL area) × 100).

Histology–OCT coregistration. Corresponding OCT frames were selected for analysis to match the pre-selected histological samples starting at the distal part of the stent. Similarly, histological sections were excised (~1.3-mm thickness) and measured, thus ensuring a high level of correlation. The locations of the OCT frames were selected by using the pullback speed and frame numbers to precisely determine the position of the in vivo image within the stent. Each of these frames was matched with the corresponding histological frame. The OCT imaging was performed in a total of 66 stents, the remainder being assigned for scanning electron microscopy analysis. Stent, lumen, and neointimal areas and neointimal thickness measurements for all stent groups were compared. Additionally, the percentage area stenosis for each frame was calculated

and compared. Linear regression analysis between the OCT and histological measurements was performed for each parameter at each time point and for each stent technology, providing an accurate assessment of the correlation between measurements.

Statistical analysis. All statistical analyses were performed using MATLAB (R2008a, The MathWorks, Natick, Massachusetts). Descriptive statistics were used for this study. All OCT measurements were tabulated as mean ± SD. Normality testing and analysis showed slight skewness within several data parameters. However, due to the Central Limit Theorem, the sample size of each parameter investigated was sufficiently large to be well approximated by a normal distribution and to justify the use of parametric hypothesis testing methods (17–19). A Student *t* test was performed to examine differences in stent, lumen, and neointimal areas; neointimal thicknesses; and the percent area stenosis by OCT and histology. Quantitative differences in neointimal area, thickness, and percentage area stenosis between groups of stents were evaluated by analysis of variance, and if a difference was found, were compared using the Dunnett test, holding Vision as the control. A value of $p < 0.05$ was considered statistically significant. The Pearson correlation coefficient was calculated to determine the level of correlation between OCT and histology per stent type at 28 and 90 days. No adjustment was made to account for correlated observations within individual animals.

Interobserver and intraobserver variability. All OCT measurements were performed by 2 experienced operators, and their results were compared to gauge the interobserver variability of the study. Two weeks later, the primary observer repeated the measurements, and these were compared with the initial observations to gauge intraobserver variability. Linear regression analysis was performed on all corresponding data sets, and the resulting squared correlation coefficient (R^2 value) was reported.

RESULTS

In vivo OCT morphometric measurements. A total of 66 stent OCT pullbacks were complete and of adequate quality for analysis. Among those, 49 pullbacks in 28 pigs were selected for comparison with histology based on the ability to match individual cross sections yielding a total of 622 analyzable OCT–histology matched images. Table 1 highlights the main differences in OCT frame-analyzed morphometric parameters at 28 and 90 days. The overall mean stent area was 6.98 ± 0.85 mm^2 at 28 days and 7.18 ± 0.92 mm^2 at 90 days. At 28 days, the detectable neointimal area ranged from a minimum of 0.09 mm^2 to a maximum of 6.76 mm^2 (mean 2.46 ± 1.97 mm^2). At this time point, the Xience V stent showed the smallest neointimal area (1.87 ± 2.09 mm^2), followed by the Taxus (2.46 ± 1.81 mm^2), Endeavor (2.50 ± 2.05 mm^2), and ML Vision (2.95 ± 1.82 mm^2) stents. However, these differences were not statistically significant when compared among the stent types ($p = 0.088$). At 90 days, the detectable neointimal area ranged from a minimum of 0.24 mm^2 to a maximum of 5.44 mm^2 (mean 2.19 ± 1.19 mm^2). At this time point, the ML Vision stents displayed the smallest neointimal area (1.58 ± 0.77 mm^2), followed by the Endeavor (1.78 ± 0.70 mm^2), Xience V (2.25 ± 1.35 mm^2), and Taxus (3.08 ± 1.21 mm^2) stents ($p < 0.0001$). At 28 days, the minimal detectable neointimal thickness measured by OCT was 0.010 mm and the mean neointimal thickness equaled 0.35 ± 0.27 mm. A total of 2,676 individual struts were analyzed for the presence of neointimal strut coverage. In general, the percentage of struts that were classified to be uncovered by OCT was 1.16% (0.819% of the struts at 28 days and 1.57% of the struts at 90 days). In addition, OCT described neointimal coverage <40 μm in 2.84% of the struts, whereas most (84.9%) of the strut coverage was >100 μm thick. Uncovered struts were found predominantly in the mid to

Table 1. Morphological Parameters Assessed In Vivo by OCT Frame Analysis at 28 and 90 Days

	Stent Area (mm^2) (n = 311)	Lumen Area (mm^2) (n = 311)	Neointimal Area (mm^2) (n = 311)	Neointimal Thickness (mm) (n = 286)	Area Stenosis (%) (n = 311)
All	7.0770 ± 0.8913	4.7397 ± 1.7648	2.3352 ± 1.6486	0.3251 ± 0.2278	33.2252 ± 22.6060
28 days	6.9815 ± 0.8521	4.5173 ± 1.9891	2.4642 ± 1.9718	0.3527 ± 0.2714	35.2159 ± 26.8673
90 days	7.1809 ± 0.92373	4.9815 ± 1.4513	2.1949 ± 1.1939	0.2890 ± 0.1469	31.0609 ± 16.6159
p value	<0.05	<0.05	0.150	<0.05	0.105

Values are mean ± SD unless indicated otherwise.
OCT = optical coherence tomography.

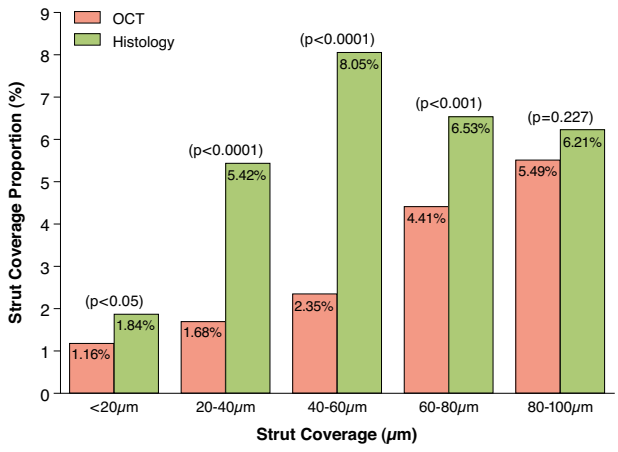

Figure 1. Distribution of Neointimal Thickness Among 6,640 Individual Stent Struts Assessed by OCT (2,676 Struts) and Histology (3,964 Struts)

Both OCT and histology detected similar proportions of uncovered struts, different proportions of struts with 20 to 80 μm of coverage, and similar proportions with 80 to 100 μm of coverage. OCT = optical coherence tomography.

proximal sections of the stents, with 40.08% of uncovered struts located in the proximal 4 mm, 35.60% located in the mid 4 mm, and 24.32% located in the distal 4 mm of the stent. Linear regression analyses showed very low intraobserver variability for stent, lumen, and neointimal areas, as well as for neointimal thicknesses as measured by OCT (R^2 = 0.958, 0.992, 0.98, and 0.975, respectively). Similarly, interobserver variability was very low (R^2 = 0.917, 0.993, 0.97, and 0.962, respectively).

OCT–histology comparison. Table 2 shows the main differences between the morphometric variables measured by OCT frame and histological slide analysis. Overall, the mean stent area measurement by OCT was 6.1% greater than measured by histology (OCT 7.08 ± 0.89 mm^2 vs. histology 6.67 ± 0.97 mm^2, $p < 0.0001$). The smallest variation in stent area was seen with the Endeavor stent (mean stent area by OCT 7.26 ± 0.93 mm^2 vs. histology 7.29 ± 0.74 mm^2, p = NS). The overall mean lumen area measured by OCT was 13.7% greater than measured by histology (4.74 ± 1.77 mm^2 vs. 4.17 ± 1.64 mm^2, respectively, $p < 0.0001$). All stent types were found to have consistently larger lumen areas by OCT compared with histology (ML Vision 20.76%, Xience V 14.33%, Endeavor 10.89%, Taxus 8.77% variation, $p < 0.0001$ for all). In addition, the mean neointimal area measurement by histology was 6.88% greater than that measured by OCT (2.50 ± 1.38 mm^2 vs. 2.34 ± 1.65 mm^2, respectively, $p < 0.001$). The mean neointimal thickness by OCT was found to be slightly (3.27%) greater than that measured by histology (0.3251 ± 0.2278 mm vs. 0.3148 ± 0.2292 mm, respectively, p = NS). Similarly, when strut coverage measurements were stratified according to thickness and a strut-by-strut analysis was performed (OCT, n = 2,676 struts; histology, n = 3,964 struts), it was shown that the presence of uncovered struts was similarly detected by each technique (1.16% OCT vs. 1.84% histology). However, the proportion of stent struts covered by >20 μm of neointimal thickness varied when assessed by OCT and histology (Fig. 1).

Figure 2 shows linear regression analyses for the main morphometric parameters analyzed by OCT correlated to histology. In general, the matched comparison between OCT and histological stent areas showed only a poor correlation regardless of the stent type (R^2 = 0.352). At 90 days, the correlation marginally improved compared with 28 days, but was still poor and independent of the stent design. Correlation of matched lumen area measurements was high (R^2 = 0.825). This high correlation was maintained at 28 and 90 days and was also independent of stent type (Fig. 3). Correlation of matched neointimal area measurements was high overall (R^2 = 0.804), as was correlation of thickness measurements overall (R^2 = 0.789) and at 28 (R^2 = 0.917) and 90 (R^2 = 0.708) days.

Table 2. Comparison of Arterial Morphological Parameters as Assessed In Vivo by OCT Frame Analysis and Ex Vivo by Histological Slide Analysis

	OCT	Histology	Delta, %	p Value
Stent area (mm^2, n = 311)	7.077 ± 0.8913	6.670 ± 0.96862	6.1019	<0.0001
Lumen area (mm^2, n = 311)	4.7397 ± 1.7648	4.1686 ± 1.6357	13.7	<0.0001
Neointimal area (mm^2, n = 311)	2.3352 ± 1.6486	2.4958 ± 1.3814	6.4348	<0.001
Neointimal thickness (mm, n = 286)	0.3251 ± 0.2278	0.3148 ± 0.2292	3.2719	0.11
Area stenosis (%, n = 311)	33.2252 ± 22.606	38.2644 ± 20.7668	13.1694	<0.0001

Values are mean ± SD.
OCT = optical coherence tomography.

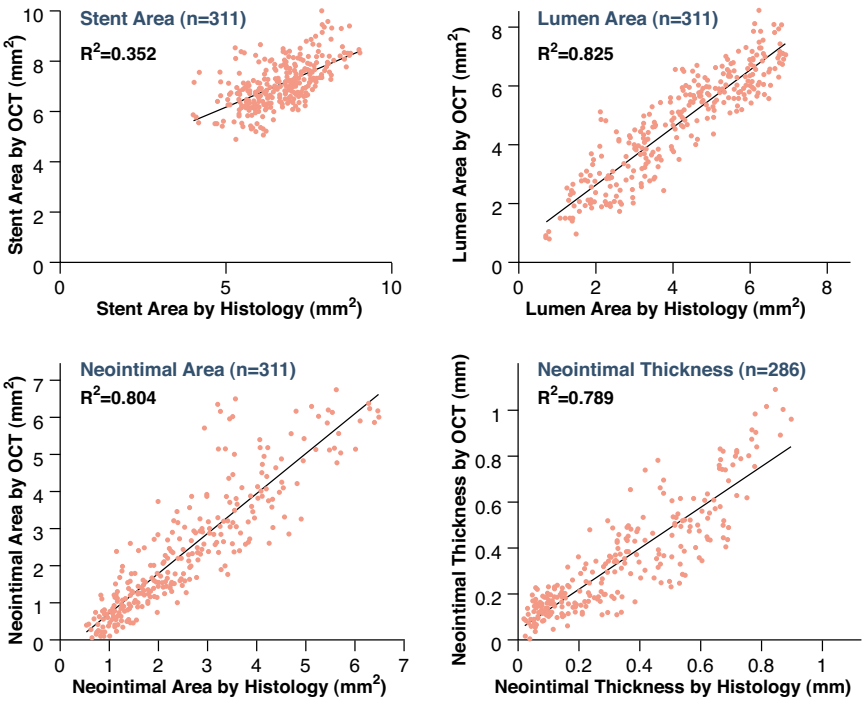

Figure 2. OCT Frame

Histological slide correlation analysis combining all 4 stents groups and showing good correlation for lumen area, neointimal area, and neointimal thickness, but poor correlation for stent area. OCT = optical coherence tomography.

Likewise, matched comparisons of percentage area stenosis measurements were excellent overall (R^2 = 0.879). When considered by stent type, the correlation was excellent at 28 days (Vision = 0.951, Xience V = 0.923, Endeavor = 0.969, and Taxus = 0.974) and 90 days (Vision = 0.858, Xience V = 0.953, Endeavor = 0.917, and Taxus = 0.910).

DISCUSSION

Drug-eluting stent implantation remains the most common procedure among patients undergoing percutaneous coronary intervention (1–3). Pathology observations suggest that as a consequence of delayed neointimal response, uncovered struts may remain for years after the implantation of these devices. It is believed that the continuous presence of exposed pro-thrombotic stent and polymer material could be an important etiological factor in the genesis of late stent thrombosis (7,20). Compared with histology, OCT is performed in vivo, allowing for the quantification of morphometric stent parameters at multiple time points across the entire stent length unmarred by artifacts and distortions due to histological cutting.

Because of its high resolution and image quality, OCT is highly suited for the evaluation of strut coverage, and potentially for the identification of patients at risk of late thrombotic events (8–16). In the present study, we examined the accuracy and reproducibility of OCT in quantifying the degree of neointimal formation after DES implantation in an experimental setting. Several contemporaneous DES technologies were used in the study, and their neointimal responses were evaluated by OCT and compared with corresponding histological specimens. To the best of our knowledge, this is the first histological validation study of the ability of OCT to probe differences in neointimal response among multiple stents at varying time points.

We found that most of the morphological characteristics analyzed were slightly magnified by OCT when compared with histology. The OCT measurements of stent area were on average approximately 6.1% greater than the same measurements by histology, and this trend was apparent within all stent types. Similarly, the lumen area measurements by OCT were on average 13.7% greater than the same measurements by histology, and this trend also was present across the 4 stent technologies.

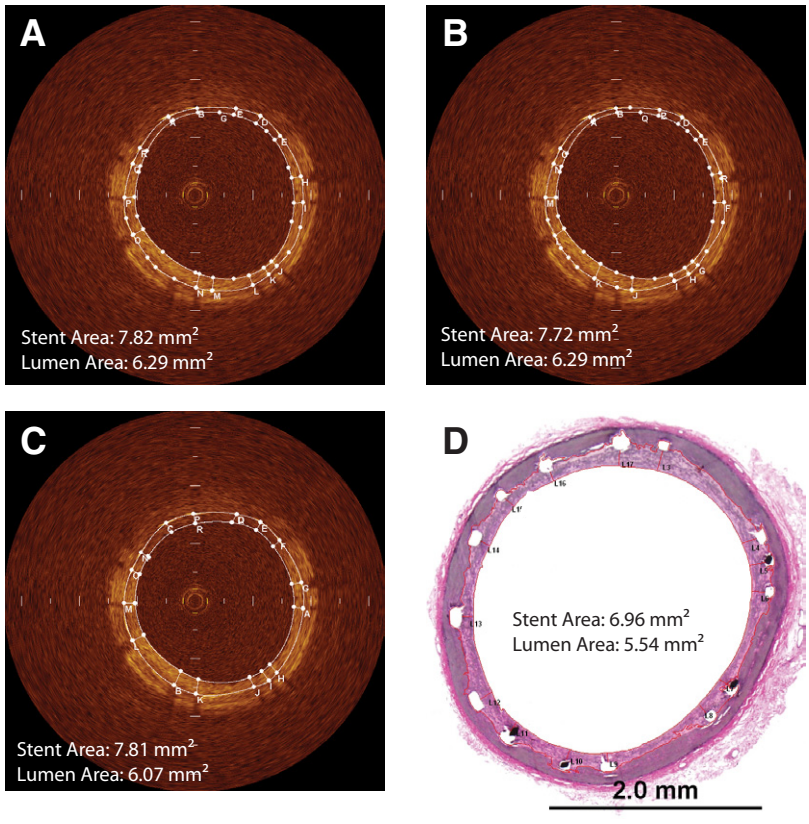

Figure 3. Representative Examples of OCT and Histology Correlation

Examples of intraobserver (Observer 1) **(A and B)** and interobserver (Observer 2) **(C)** correlation in stent and lumen measurements as assessed in vivo by OCT. Corresponding hematoxylin and eosin–stained histological cross section showing accurate coregistration of OCT frames with excised tissue **(D)**. OCT = optical coherence tomography.

Finally, percentage area stenosis was on average 5.4% greater by histology than by OCT, with all stent types following a similar trend. Although most of the differences seen in the morphometric measurements between OCT and histology may be explained by tissue shrinkage due to histological processing, technical issues also may have contributed to the overestimation of the values. It is possible that light attenuation within the arterial tissue resulted in a lack of stent strut definition in large vessels, leading to overestimation of some of the measurements.

In particular, the near field structures (neointimal area and thickness) seemed to have the highest degree of accuracy. In our study, OCT was able to detect different degrees of neointimal thickening within all of the 286 stent cross sections measured. Within these sections, 28.1% of stent struts were covered by a thin neointimal thickening <150 μm, the resolution threshold of the current gold standard of invasive imaging, intravascular ultrasound. Thus, there is a clear advantage in using OCT for the detection of miniscule tissue coverage hitherto undetectable by invasive imaging. The measurement of near field structures by OCT also correlated exceptionally well with histology. Typically, the neointimal thickness fell within the depth attenuation limitation of the technology, and unlike measurements of stent area, is quantified without obfuscation due to nearby stent struts. Likewise, percentage area stenosis measurements by OCT and histology showed excellent correlation. The ability of OCT to distinguish the luminal border was apparent given the high correlation of lumen area measurements by OCT and histology. As shown by the good correlation between OCT and histological lumen area across stent types, the proximity of the OCT transducer to the vessel wall and the evacuation of blood due to saline flush provided for a clear view of the luminal border, making measurement accurate and highly reproducible. However, in any case, in this study OCT showed a very low intraobserver and interobserver variability

($R^2 > 0.9$) in the evaluation of all morphometric parameters evaluated.

In our study, morphometric differences at the strut level were easily discerned. In this particular analysis, OCT and histology detected a similar proportion (1.16% and 1.84%) of uncovered struts. However, the proportions of struts displaying neointimal thicknesses ranging from 20 to 80 μm differed significantly between OCT and histology. Particularly, this difference was marked between the 20- and 60-μm range. These proportions converged for neointimal coverage between 80 and 100 μm. Finally, OCT determined a greater proportion of struts covered by >100 μm of tissue than histology (84.90% and 71.95%). Hence, OCT seems to correlate appropriately with histology in either the absence (<20 μm) or the presence (>100 μm) of robust neointima; however, the correlation does not seem to be very linear in between these values (Fig. 1). A possible explanation for these findings is that the potential for accurate observer assessment is greatest both in the complete absence of neointima and in the presence of a robust amount of neointima covering the strut. Hence, the largest variation of neointima evaluation may occur within these boundaries as a consequence of artifacts, OCT resolution issues, and independent observer interpretation.

Although histology showed differences in neointimal composition, OCT was unable to distinguish between fibrin, giant cells, granulomatous reaction, and degree of endothelialization, and thus it serves best as a morphological tool rather than one for the characterization of tissue types.

Due to its high resolution, OCT has been shown to produce consistently high-quality, reliable images. However, because a flushing OCT system was used in the current study, animal hearts are hyperdynamic, and normal coronary arteries are more challenging to image, some of the OCT frames had to be excluded. Because the objective of the study was to find appropriate OCT–histology matched frames, approximately 21% of the OCT frames did not meet criteria for inclusion due to inadequate quality, presence of artifacts, or poor landmarks, prohibiting histological correlation.

In the present study, although the mean difference in stent areas measured by OCT was found to be only 6.1% greater than that measured by histology, the overall correlation was generally low compared with the high correlation shown in lumen and neointimal areas. We believe that image wire tilt during imaging could be one of the mechanisms responsible for these findings. Due to the small size and extreme flexibility of the image wire, tilting while imaging has been known to occur. Images generated by an optical source positioned at an angle nonperpendicular to the artery center could result in systemic bias toward larger OCT areas. An independent correlation of the individual differences between OCT and histological stent areas and the OCT measurements themselves shows a trend toward greater differences as the stent area increases (graph not shown). In addition, the shrinkage artifact caused during histology processing and differences in the technique used to measure total stent area between OCT and histology may have contributed to the differences found.

The accuracy of matching histological tissue with corresponding images acquired in vivo remains a significant challenge to the validation of many imaging modalities. Although the greatest care was taken to ensure precise colocation of OCT frames and histological sections, it is possible that inherent limitations therein, as well as catheter shift due to cardiac motion, played a role in the poor correlation of stent area measurements in this study. Furthermore, strut damage due to cutting during the tissue preparation process could have exacerbated this finding. Examination of neointimal coverage by OCT must factor in adjustment for strut blooming, the unclear delineation of the stent strut surface due to its hyper-reflectivity. Typically, the strut blooming is about 37 μm in thickness and extends bidirectionally toward and away from the catheter light source, complicating the measurement of low neointimal coverage (<20 μm). We avoided potential error by measuring neointimal thickness from the center of the blooming artifact to the luminal border toward the arterial center of gravity. We believe this practice resulted in the high correlation between OCT and histological measurements of neointimal thickness overall. Therefore, OCT may prove to be a more appropriate tool for the assessment of fine, near microstructures, such as thrombus or neointimal coverage, than for the accurate measurement of deployed stent area. Although increases in the pullback speed and enhancements in the frame acquisition rate in future OCT technology should mitigate the concerns of balloon occlusion, we do not expect significant changes in image quality to invalidate our present findings.

At the present time, challenges still remain for the future implementation of current OCT technology in the clinical setting. Mainly, the limited penetration of OCT may affect the ability to dis-

JACC: CARDIOVASCULAR IMAGING, VOL. 3, NO. 1, 2010
JANUARY 2010:76–84

tinguish stent struts distant to the transducer. Because light cannot pass though the metallic stent struts, but is instead almost completely reflected, strut surfaces have an enhanced reflectivity with shadowing that obscures the tissue behind them.

In summary, OCT is a reliable and highly reproducible method for the evaluation of overall neointimal formation after stent implantation. In addition, this technique seems to be able to accurately discern the percentage of struts covered by neointimal formation. However, although OCT seems to be very accurate in evaluating uncovered struts, it shows some variability in the quantification of neointimal thickness at the strut level when ranging between 20 and 80 μm, showing greater certainty when evaluating thicknesses above 80 μm. The evaluation of the stent area seems to be more difficult to discern, and further research is needed to clarify the significance of this finding.

Reprint requests and correspondence: Dr. Juan F. Granada, Skirball Center for Cardiovascular Research, Cardiovascular Research Foundation, 8 Corporate Drive, Orangeburg, New York 10962. *E-mail: jgranada@crf.org.*

REFERENCES

1. Stone GW, Moses JW, Ellis SG, et al. Safety and efficacy of sirolimus- and paclitaxel-eluting coronary stents. N Engl J Med 2007;356:998–1008.
2. Spaulding C, Daemen J, Boersma E, Cutlip DE, Serruys PW. A pooled analysis of data comparing sirolimus-eluting stents with bare-metal stents. N Engl J Med 2007;356:989–97.
3. Kastrati A, Mehilli J, Pache J, et al. Analysis of 14 trials comparing sirolimus-eluting stents with bare-metal stents. N Engl J Med 2007;356:1030–9.
4. Bavry AA, Bhatt DL. Appropriate use of drug-eluting stents: balancing the reduction in restenosis with the concern of late thrombosis. Lancet 2008;371:2134–43.
5. Moreno R, Fernandez C, Hernandez R, et al. Drug-eluting stent thrombosis: results from a pooled analysis including 10 randomized studies. J Am Coll Cardiol 2005;45:954–9.
6. Nakazawa G, Finn AV, Joner M, et al. Delayed arterial healing and increased late stent thrombosis at culprit sites after drug-eluting stent placement for acute myocardial infarction patients: an autopsy study. Circulation 2008;118:1138–45.
7. Luscher TF, Steffel J, Eberli FR, et al. Drug-eluting stent and coronary thrombosis: biological mechanisms and clinical implications. Circulation 2007;115:1051–8.
8. Bouma BE, Tearney GJ, Yabushita H, et al. Evaluation of intracoronary stenting by intravascular optical coherence tomography. Heart 2003;89:317–20.
9. de Smet BJGL, Zijlstra F. A look at drug eluting stents with optical coherence tomography. Eur Heart J 2007:28:918–9.
10. Kume T, Akasaka T, Kawamoto T, et al. Visualization of neointima formation by optical coherence tomography. Int Heart J 2005;46:1133–6.
11. Matsumoto D, Shite J, Shinke T, et al. Neointimal coverage of sirolimus-eluting stents at 6-month follow-up: evaluated by optical coherence tomography. Eur Heart J 2007;28:961–7.
12. Takano M, Inami S, Jang IK, et al. Evaluation by optical coherence tomography of neointimal coverage of sirolimus-eluting stent three months after implantation. Am J Cardiol 2007;99:1033–8.
13. Suzuki Y, Ikeno F, Koizumi T, et al. In vivo comparison between optical coherence tomography and intravascular ultrasound for detecting small degrees of in-stent neointima after stent implantation. J Am Coll Cardiol Intv 2008;1:168–73.
14. Guagliumi G, Sirbu V. Optical coherence tomography: high resolution intravascular imaging to evaluate vascular healing after coronary stenting. Catheter Cardiovasc Interv 2008;72:237–47.
15. Chen BX, Ma FY, Luo W, et al. Neointimal coverage of bare-metal and sirolimus-eluting stents evaluated with optical coherence tomography. Heart 2008;94:566–70.
16. Kawase Y, Hoshino K, Yoneyama R, et al. In vivo volumetric analysis of coronary stent using optical coherence tomography with a novel balloon occlusion-flushing catheter: a comparison with intravascular ultrasound. Ultrasound Med Biol 2005;31:1343–9.
17. Boneau CA. The effects of violations of assumptions underlying the t test. Psychol Bull 1960;57:49–64.
18. Stonehouse JM, Forrester GJ. Robustness of the t and U tests under combined assumption violations. J Appl Statistics 1998;25:63–74.
19. Lumley T, Diehr P, Emerson S, Chen L. The importance of the normality assumption in large public health data sets. Annu Rev Public Health 2002;23:151–69.
20. Nakazawa G, Finn AV, Ladich E, et al. Drug-eluting stent safety: findings from preclinical studies. Expert Rev Cardiovasc Ther 2008;6:1379–91.

Key Words: optical coherence tomography ■ imaging validation ■ drug-eluting stent.